Journal of Solid State Chemistry 183 (2010) 1150–1158

Contents lists available at ScienceDirect

Journal of Solid State Chemistry

journal homepage: www.elsevier.com/locate/jssc

Two anionic $[Cu_6^{I}X_7]_n^{n-}$ (X=Br and I) chain-based organic–inorganic hybrid solids with *N*-substituted benzotriazole ligands

Xia Gao, Quan-Guo Zhai, Shu-Ni Li, Rui Xia, Hai-Juan Xiang, Yu-Cheng Jiang, Man-Cheng Hu *

Key Laboratory of Macromolecular Science of Shaanxi Province, School of Chemistry and Materials Science, Shaanxi Normal University, Xi' an, Shaanxi 710062, PR China

ARTICLE INFO

Article history:
Received 8 November 2009
Received in revised form
1 March 2010
Accepted 8 March 2010
Available online 12 March 2010

Keywords:
CuI
CuBr
N-Ethylbenzotriazole
1,6-Bi(benzotriazole)hexane
Organic–inorganic hybrid solid

ABSTRACT

Solvothermal reactions of the flexible ligand 1,6-Bi(benzotriazole)hexane with CuI and KI or CuBr and KBr in ethanol generate two hybrid compounds, namely, $\{(HETA)[(Cu_6I_7)(ETA)_2]\}_n$(**1**) and $\{K(Cu_6Br_7)(BBTH)\}_n$(**2**) (ETA=*N*-ethylbenzotriazole, HETA=protonated *N*-ethylbenzotriazole, BBTH=1,6-bi(benzotriazole)hexane). In **1**, two $[Cu_3I_4]$ vertex missing cubane-like subunits link each other by sharing one I atom to give a $[Cu_6I_7]$ cluster, which further form novel 1D $[Cu_6I_7]_n^{n-}$ anionic chain. Two in-situ generated ETA ligands finished the 4-coordinated environments of copper centers and another one discrete protonated ETA ligand keeps the charge neutrality for **1**. In complex **2**, bowl-shaped $[Cu_5Br_4]$ clusters and rhomboid $[Cu_2Br_2]$ dimers link each other to generate a $[Cu_6Br_7]_n^{n-}$ 1D chain. BBTH ligands complete the tetrahedral spheres of Cu(I), and 7-coordinated K atoms further extend the 1D chain motifs to a 2D hybrid layer of **2**. The UV–vis diffuse reflectance spectrum and luminescence measurements show that compound **1** and **2** both are potential semiconductor and photoluminescence materials.

1. Introduction

The current increasing attention and powerful driving force in the organic–inorganic hybrid materials not only originate from their fascinating properties in material science, medicine, catalysis, etc., but also from their intriguing variety of architectures and their diversity of electronic structures and topologies [1–11]. In those materials, the inorganic component may confer useful optical or magnetic properties and thermal stability, while the organic component offers the potential for a range of polarizabilities and structural diversification. The combination of these two kinds of components results in the characteristics of diverse structural chemistry and novel physical properties [12–16].

Among these types of hybrid compounds reported so far, copper(I) halides have been widely investigated due to their rich photoluminescent properties and intriguing topology [17,18]. Copper(I) tends to form a variety of coordination compounds with halides, ranging from 0D complexes to 3D frameworks with structural moieties such as rhomboid $Cu_{2\times2}$ dimers, cubane or step-cubane $Cu_{4\times4}$ tetramers, zigzag $[CuX]_n$ chains, and hexagonal $[Cu_{6\times6}]_n$ grid chains [19–24]. It should be noted that the rich structural variation in the $[(Cu_aX_b)^{a-b}]_n$ species is basically caused by the ligating versatility of the halide anions, constructing diverse neutral ($a=b$), cationic ($a>b$) and anionic ($a<b$) aggregates. In contrast to the extensively investigated neutral species, the structural and luminescent aspects of anionic or cationic copper (I) halide aggregates remain rarely explored due to synthetic and calculating difficulties [25–30]. On the other hand, organic species, with versatile binding modes and features can be used to transfer energy or electron, enhance spinorbital coupling as well as impart chemical reactivity or chirality [23,24,31–37]. As a result, rigid or flexible multidentate nitrogen-donor ligands usually act as organic connectors to link these copper halide motifs to form extended organic–inorganic hybrid architectures. Thus, the design of organic ligands is a useful way of manipulating the hybrid structures.

In the context of our research interest on the coordination chemistry of polyazaheteroaromatic ligands, we recently reported on the influence of the spacer length of α,ω-bis(benzotriazole)-alkane organic ligands on the solid state structures of CuX-based hybrid coordination polymers. Novel $\{Cu_{3\times3}\}_n$ ladder-like chain and $\{Cu_{8\times8}\}_n$ ribbons have been firstly presented [24]. Moreover, the increasing dimensionality from 1-D to 3-D indicates that the spacer length and isomerism of the bis(benzotriazole)alkane ligands play an essential role in formation of the framework of these hybrid materials. In order to further our investigations, 1, 6-bi(benzotriazole)hexane (BBTH) with much longer alkane spacer is selected. To the best of our knowledge, neither hydro(solvo)thermal nor solution methods have been used to synthesize any compounds containing BBTH ligand. In other words, no investigation about hybrid materials constructed from

* Corresponding authors. Fax: +86 29 85307774.
E-mail addresses: zhaiqg@snnu.edu.cn (Q.-G. Zhai), hmch@snnu.edu.cn (M.-C. Hu).

0022-4596/$ - see front matter © 2010 Elsevier Inc. All rights reserved.
doi:10.1016/j.jssc.2010.03.007

BBTH ligand has been reported to date. Herein, using BBTH ligand under solvothermal reactions with CuI and KI or CuBr and KBr in ethanol generate two novel hybrid compounds, namely, $\{(HETA)[(Cu_6I_7)(ETA)_2]\}_n$ (**1**) and $\{K(Cu_6Br_7)(BBTH)\}_n$ (**2**) (ETA= *N*-ethyl-benzotriazole, HETA=protonated *N*-ethylbenzotriazole, BBTH=1,6-bi(benzotriazole)-hexane). Furthermore, these two compounds have been characterized by X-ray single-crystal diffractions, X-ray powder diffractions (XRPD), FT-IR, elemental analysis, TG/DTA, UV-vis diffuse reflectance spectra, and solid-state and solution photoluminescence measurements.

2. Experimental

2.1. Materials and physical measurements

The ligand 1,6-Bi(benzotriazole)hexane was synthesized according to a literature method [38]. Other reagents and solvents employed were commercially available and used without further purification. The Fourier-transform infrared spectra (KBr pellets) were recorded using a Nicolet Avatar 360 FT–IR Spectrometer in the range of 4000–400 cm^{-1}. C, H, and N elemental analyses were performed using an Elementar Vario EL III elemental analyzer. X-ray powder diffraction data were recorded on a Rigaku Multi-Flex diffractometer with a scan speed of 0.05–0.2°/min. Thermal stability studies were carried out using a NETSCHZ STA–449C thermoanalyzer under a nitrogen atmosphere (40–1000 °C range) at a heating rate of 10 °C/min. UV–vis diffuse reflectance spectra were obtained with a Lamdba 900 UV–vis–NIR spectrophotometer at room temperature. Initially, the 100% line flatness of the spectrophotometer was set using barium sulfate ($BaSO_4$). A powder crystal sample of the compound was mounted on the sample holder. The thickness of the sample was much larger than the individual crystal particles. The solid-state and solution fluorescence spectra all were measured with a Cary Eclipse fluorescence spectrophotometer at room temperature. The excitation slit and emission slit were both 2.5 nm.

2.2. Synthesis of $\{(HETA)[(Cu_6I_7)(ETA)_2]\}_n$ (**1**)

A mixture of CuI (0.190 g, 1.0 mmol), BBTH (0.161 g, 0.5 mmol), KI (0.166 g, 1.0 mmol) and ethanol (10 mL) was stirred for 30 min in a 25 mL Teflon-lined reactor then sealed the reactor. The reactor was heated in an oven to 180 °C for 120 h and then cooled to room temperature at a rate of 2.5 °C h^{-1}. Yellow block-shaped crystals of **1** were obtained by filtration, washed with ethanol, and dried in air (Yield: ca. 0.12 g, 32% based on Cu). Anal. Calcd. (%) for $C_{24}H_{28}Cu_6I_7N_9$ (%): C 16.84, H 1.65, N 7.36; Found (%): C 17.01, H 1.58, N 7.26. FT-IR (KBr pellet, cm^{-1}): 2973(m), 2925(m), 1602(m), 1494(w), 1446(s), 1380(m), 1316(s), 1241(s), 1194(s), 1069(s), 1030(w), 750(s).

2.3. Synthesis of $\{K(Cu_6Br_7)(BBTH)\}_n$ (**2**)

A mixture of CuBr (0.215 g, 1.5 mmol), BBTH (0.161 g, 0.5 mmol), KBr (0.119 g, 1.0 mmol) and ethanol (10 mL) was stirred for 30 min in a 25 mL Teflon-lined reactor then sealed the reactor. The reactor was heated in an oven to 180 °C for 120 h and then cooled to room temperature at a rate of 2.5 °C h^{-1}. Yellow block-shaped crystals of **2** were obtained by filtration, washed with ethanol, and dried in air (Yield: ca. 0.132 g, 45% based on Cu). Anal. Calcd. (%) for $C_{18}H_{20}Cu_6Br_7KN_6$ (%): C 16.63, H 1.55, N 6.46; Found (%): C 16.72, H 1.42, N 6.50. FT-IR (KBr pellet, cm^{-1}): 3075(w), 2934(m), 2954(w), 1613(w), 1491(w), 1441(m), 1371(w), 1322(m), 1216(s), 1158(w), 1127(w), 1086(w), 997(w), 747(s).

2.4. Crystal structure determination

Suitable single crystals of **1** and **2** were carefully selected under an optical microscope and glued to thin glass fibers. Crystallographic data for all compounds were collected with a Siemens Smart CCD Diffractometer with graphite-monochromated Mo $K\alpha$ radiation (λ=0.71073 Å) at T=298(2) K. Absorption corrections were made using the SADABS program [39]. The structures were solved using the direct method and refined by full-matrix least-squares methods on F^2 by using the SHELXL-97 program package [40]. All non-hydrogen atoms were refined anisotropically. Positions of the hydrogen atoms attached to carbon and oxygen atoms were fixed at their ideal positions. Crystal data as well as details of data collection and refinements for **1** and **2** are summarized in Table 1. Selected bond lengths and angles are listed in Table 2.

3. Results and discussion

3.1. Syntheses

Complexes **1** and **2** were both synthesized by BBTH ligand, CuI and KI or CuBr and KBr in ethanol solvent with the identical reaction temperature and reaction time. However, only mono-*N*-ethylbenzotriazole ligands were found in the ultimate products of compound **1**. It is noted that the kind of anions that linked with metal cations is a key factor to affect the formation of the resulting products as well as the formation mechanism. It is well known that iodide ions are a stronger nucleophile than bromine ions. That is to say, iodine ions take place nucleophilic substitution reaction easily compared with bromine ions. On the basis of the above theory and some literature reports [19], we can tentatively speculate the formation mechanism of **1** as depicted in Scheme 1: benzotriazole acquired by the rupture of the BBTH

Table 1
Crystal data and structure refinements for compounds **1** and **2**.

Compound	**1**	**2**
Empirical formula	$C_{24}H_{28}Cu_6I_7N_9$	$C_{18}H_{20}Br_7Cu_6KN_6$
fw	1712.09	1300.11
Cryst syst	Monoclinic	Monoclinic
Space group	C2/c	$P2_1/m$
a (Å)	20.886(2)	7.9590(10)
b (Å)	11.0602(13)	19.140(2)
c (Å)	21.071(3)	10.1109(14)
α (deg)	90	90
β (deg)	109.50(2)	100.98(10)
γ (deg)	90	90
V (Å^3)	4588.2(9)	1512.0(3)
Z	4	2
T (K)	298(2)	298(2)
D_{calcd}(g cm^{-3})	2.479	2.856
μ(mm^{-1})	7.468	13.553
F(0 0 0)	3120	1216
θ for data collection (deg)	2.05–25.02	2.05–25.02
Reflections collected/unique	11 804/4038	7608/2756
R(int)	0.0707	0.0534
Parameters	257	197
GOF on F^2	0.990	1.027
R_1[a], wR_2 [$I > 2\delta$ (I)]	0.0506, 0.1342	0.0431, 0.0873
R_1, wR_2 (all data)	0.0772, 0.1510	0.0741, 0.0968
ρ_{fin}(max/min) (e Å^{-3})	1.409, −1.404	1.066, −1.054

[a] $R_1=\sum(|F_o|-|F_c|)/\sum|F_o|$, $wR_2=[\sum w(F_o^2-F_c^2)^2/\sum w(F_o^2)^2]^{0.5}$.

Table 2
Selected bond lengths [Å] and angles [°] for compounds **1** and **2**.

		1			
Cu(1)–N(3)	2.043(9)	Cu(2)–I(4)#1	2.6109(17)	Cu(3)–N(2)	2.066(9)
Cu(1)–I(1)	2.6263(16)	Cu(2)–I(1)#2	2.6404(16)	Cu(3)–I(4)	2.6130(17)
Cu(1)–I(2)	2.6501(18)	Cu(2)–I(1)	2.7016(17)	Cu(3)–I(2)#1	2.6465(17)
Cu(1)–I(3)	2.6677(14)	Cu(2)–I(2)	2.7479(17)	Cu(3)–I(3)	2.7557(16)
N(1)–C(2)	1.372(14)	N(4)–C(15)	1.44(6)	N(2)–N(3)	1.291(12)
N(1)–C(7)	1.458(16)	N(6)–C(9)	1.38(6)	N(4)–N(5)	1.44(5)
N(3)–C(1)	1.376(13)	C(15)–C(16)	1.50(5)	N(5)–N(6)	1.44(6)
N(4)–C(10)	1.50(6)	N(1)–N(2)	1.366(13)		
N(3)–Cu(1)-I(1)	112.7(3)	I(4)#1–Cu(2)–I(1)#2	114.42(6)	N(2)–Cu(3)–I(4)	112.4(3)
N(3)–Cu(1)-I(2)	101.4(3)	I(4)#1–Cu(2)–I(1)	112.58(6)	N(2)–Cu(3)–I(2)#1	108.4(3)
I(1)–Cu(1)-I(2)	117.90(6)	I(1)#2–Cu(2)–I(1)	106.40(5)	I(4)–Cu(3)–I(2)#1	111.86(6)
N(3)–Cu(1)-I(3)	103.0(3)	I(4)#1–Cu(2)–I(2)	108.76(6)	N(2)–Cu(3)–I(3)	101.5(3)
I(1)–Cu(1)-I(3)	107.47(6)	I(1)#2–Cu(2)–I(2)	102.18(6)	I(4)–Cu(3)–I(3)	111.56(6)
I(2)–Cu(1)-I(3)	113.38(6)	I(1)–Cu(2)–I(2)	112.09(6)	I(2)#1–Cu(3)–I(3)	110.68(6)
Symmetry transformations used to generate equivalent atoms: #1—x, y, $-z+1/2$; #2—x, $-y+1$, $-z$.					
		2			
Cu(1)–N(3)	1.999(6)	Cu(3)–Br(4)#2	2.3829(16)	K(1)–Br(5)#5	3.553(3)
Cu(1)–Br(3)#1	2.4708(14)	Cu(3)–Br(5)	2.3921(16)	C(7)–N(1)	1.454(9)
Cu(1)–Br(3)	2.4926(14)	Cu(3)–Br(3)#3	2.5745(17)	C(7)–C(11)#2	1.54(5)
Cu(1)–Br(4)	2.6704(15)	Cu(3)–Br(2)	2.7912(19)	C(8)–C(9)	1.52(4)
Cu(2)–N(2)	2.035(6)	K(1)–Br(1)	3.183(3)	C(9)–C(10)	1.529(18)
Cu(2)–Br(1)	2.4031(14)	K(1)–Br(2)#5	3.316(3)	C(10)–C(11)	1.51(4)
Cu(2)–Br(4)	2.5017(15)	K(1)–Br(3)#4	3.5053(14)		
Cu(2)–Br(2)	2.6510(16)	K(1)–Br(4)	3.619(2)		
N(3)–Cu(1)–Br(3)#3	119.54(19)	N(2)–Cu(2)–Br(1)	124.11(18)	Br(4)#1–Cu(3)–Br(5)	125.29(7)
N(3)–Cu(1)–Br(3)	113.04(19)	N(2)–Cu(2)–Br(4)	102.20(18)	Br(5)–Cu(3)–Br(3)#4	104.02(6)
Br(3)#3–Cu(1)–Br(3)	110.48(5)	Br(1)–Cu(2)–Br(4)	113.49(6)	Br(4)#1–Cu(3)–Br(2)	109.13(6)
N(3)–Cu(1)–Br(4)	100.62(19)	N(2)–Cu(2)–Br(2)	106.52(18)	Br(5)–Cu(3)–Br(2)	100.97(6)
Br(3)#3–Cu(1)–Br(4)	107.00(5)	Br(1)–Cu(2)–Br(2)	100.01(5)	Br(3)#4–Cu(3)–Br(2)	101.44(5)
Br(3)–Cu(1)–Br(4)	104.33(5)	Br(4)–Cu(2)–Br(2)	110.03(5)	Br(4)#1–Cu(3)–Br(3)#4	112.97(6)
Symmetry transformations used to generate equivalent atoms: #1—x, $-y+1/2$, z; #2—$x-1$, y, z; #3—x, $-y$, $-z$; #4—x, $y+1/2$, $-z$; #5—$x+1$, y, z.					

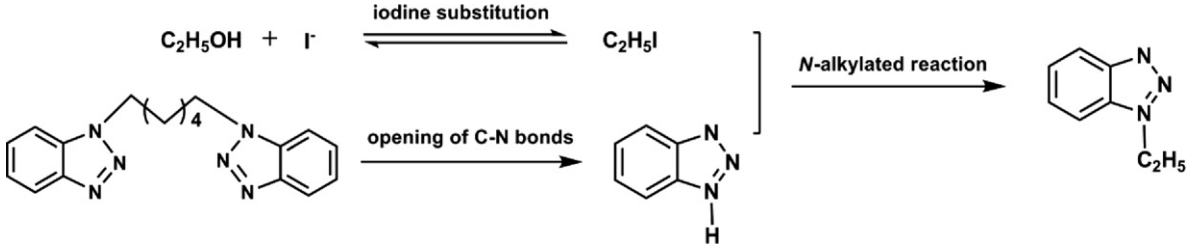

Scheme 1. Suggested mechanism of the in-situ generation of ETA ligands in 1 under solothermal reaction.

ligand while C_2H_5I formed by the nucleophilic substitution reaction of strong nucleophilic iodine ions and ethanol solvent under high temperature and autogenous pressure, both of which react to produce mono-*N*-alkylated heterocycles simultaneously. The reactants and in-situ mono-*N*-ethylbenzotriazole ligand self-assemble to produce hybrid coordination polymer **1** by the effects of kinetic and thermodynamic stabilities. The solvothermal reactions are simultaneous C–N bond rupture, *N*-alkylated and self-assembly processes, which is similar to the situation previously reported by Wu et al. [19] and Yao et al. [41]. When bromides were used instead of iodides under the same reaction conditions, we successfully synthesized complex **2**, a unique hybrid solid with BBTH ligands. To the best of our knowledge, coordination polymers based on the ligand reported here is exclusive to date.

3.2. Description of crystal structures

X-ray single-crystal diffraction analysis shows that complex **1** crystallizes in the monoclinic space group *C*2/*c*, and shows a supramolecular structure consisting of 1D anionic organic–inorganic hybrid $[(Cu_6I_7)(ETA)_2]_n^{n+}$ chains and disordered protonated HETA organic cations. As shown in Fig. 1, there exist three independent four-coordinated copper centers. The coordination environment around Cu(1) is completed by three iodine atoms and one nitrogen atom from ETA ligand, with the distances Cu(1)–N(3)=2.043(9) Å, Cu(1)–I(1)=2.6263(16) Å, Cu(1)–I(2)=2.6501(18) Å and Cu(1)–I(3)=2.6677(14) Å, respectively. The corresponding bond angles around Cu(1) are in the range of 101.4(3)–117.90(6)°. The Cu(2) atom coordinated by four iodine atoms with the Cu–I bonds are of 2.6109(17)–2.7479(17) Å, and the corresponding bond angles are in the range of 102.18(6)–114.42(6)°. Just like Cu(1), the residue Cu(3) center is also tetracoordinated to three iodine atoms and one nitrogen atom from ETA ligand (Cu(3)–N(2)=2.066(9) Å, Cu(3)–I=2.6130(17)–2.7557(16) Å). The corresponding bond angles are in the range of 101.5(3)–121.4(3)°. As depicted in Fig. 2, three independent Cu^+ and four I^- atoms link each other to form a unique vertex missing cubane-like $[Cu_3I_4]$ subunit. The Cu–Cu distances are in the range of 2.683(2)–2.7632(19) Å, which are comparable to those found in the structurally characterized compounds based on $[Cu_4I_4]$

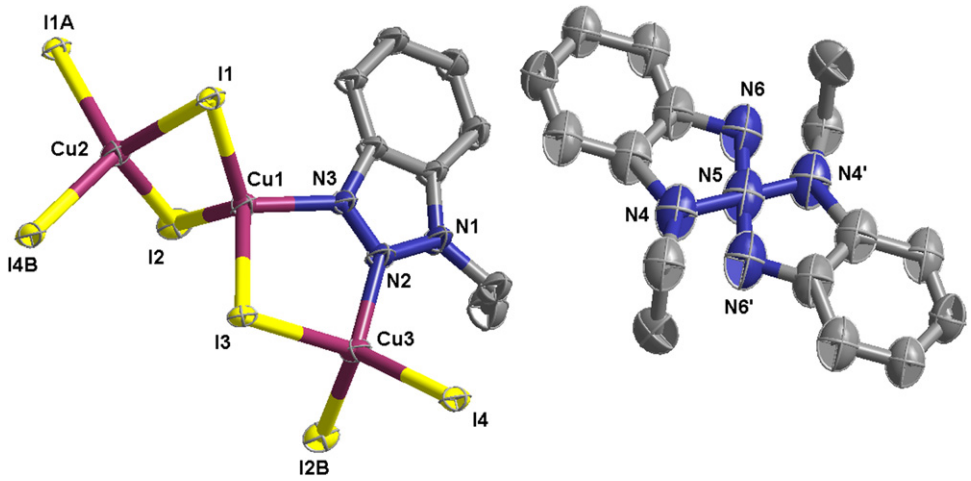

Fig. 1. View of the coordination environments of the copper atoms in compound **1** [Symmetry codes: A,—*x*, 1–*y*, –*z*; B,—*x*, *y*, 0.5–*z*].

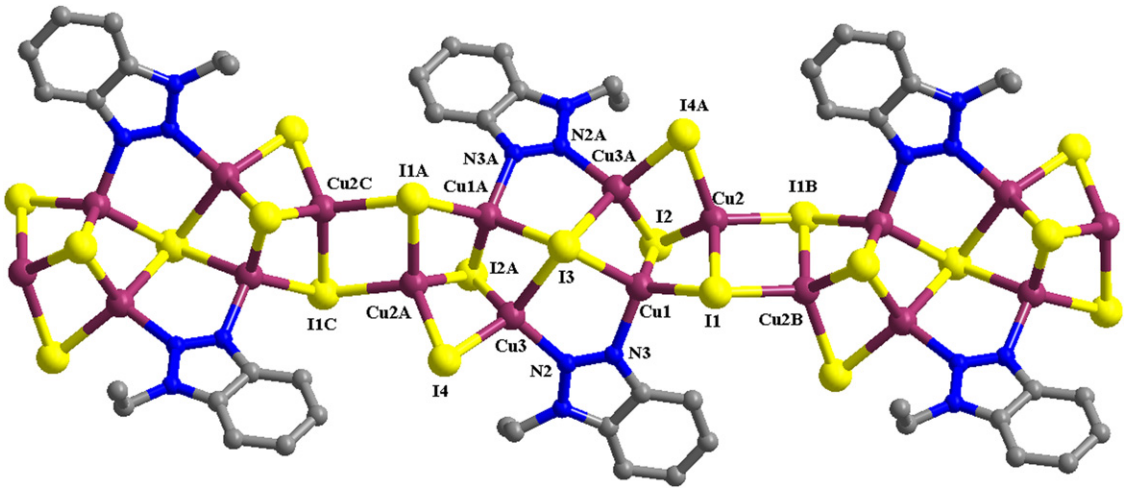

Fig. 2. View of the 1D organic–inorganic hybrid chain in compound **1**.

cubane-like clusters [24,42–45]. Two $[Cu_3I_4]$ subunits are connected by a joint I(3) atom, forming a $[Cu_6I_7]$ unit, which further link each other to construct a 1D inorganic chain structure. It is noted that adjacent $[Cu_6I_7]$ motifs take the *anti*-conformation, using Cu(2) and I(1) atoms to form a $[Cu_2I_2]$ parallelogram and the distance between diagonal copper atoms is about 3.2 Å. Thus, four independent iodine atoms are of three kinds of bridging modes: μ_2–I(4), μ_3–I(1), μ_3–I(2) and μ_4–I(3). To the best of our knowledge, this anionic $[Cu_6I_7]_n^{n-}$ inorganic chain is unprecedented in the chemistry of copper halides. Moreover, the residual coordination positions of Cu(1) and Cu(3) are occupied by two nitrogen atoms from the same ETA ligand to form the organic–inorganic hybrid anionic chain structure of compound **1** (Fig. 2). This linkage generates $[Cu_2N_2I]$ five-membered rings with copper separations of about 3.56 Å, which effectively 'ease' the repulsion of metal ions and is usually found for many triazoles of which the N_4-position is substituted [46]. The hybrid $[(Cu_6I_7)(ETA)_2]_n^{n+}$ chains are packed via very weak π–π interactions (center-to-center distance between benzotriazole rings of about 4.3 Å) to give a 3D porous supramolecular framework with channel dimensions of about 12×19 Å^2, which is fully occupied by the disordered HETA organic cations (Figure S1).

The use of bromides generated complex **2,** which crystallizes in the monoclinic space group $P2_1/m$ and contains three independent copper(I) atoms, one K atom, five bromine anions and half of BBTH ligand. As shown in Fig. 3, the Cu(1) center is tetracoordinated to three bromine atoms and one nitrogen atom from BBTH ligand, with the distances of Cu–N = 1.999(6) Å and Cu–Br = 2.4708(14)–2.6704(15) Å, respectively. The corresponding bond angles around Cu(1) are in the range of 100.62(19)–119.54(19)°. The Cu(2) atom also coordinates to three Br atoms and one N atom from benzotriazole (Cu–N = 2.035(6) Å, Cu–Br = 2.4031(14)–2.6510(16) Å, N/Br–Cu–Br = 100.01(5)–124.11(18)°). The residue 4-coordinated tetrahedral Cu(3) atom are linked to four Br atoms with Cu–Br bonds and Br–Cu–Br angles of 2.3829(16)–2.7912(19) Å and 100.97(6)–125.29(7)°. Moreover, with regard to the unique K atom, it is common heptacoordinated to seven bromine atoms. The K–Br bond lengths are in the range of 3.183(3)–3.619(2) Å and the corresponding bond angles are in the range of 66.99(2)–157.24(8)°. Two Cu(2) and two Cu(3) centers are firstly linked by five Br atoms (one Br(1), one Br(2), two Br(4) and one Br(5)) to give a novel bowl-shaped $[Cu_4Br_5]^-$ anionic motif, which can also be regarded as four neutral $[Cu_2Br_2]$ units linking each other through sharing one μ_4–Br(2) atoms. The bowl size is about 6×5 Å^2 and neighbor Cu centers are separated for 2.9413(17)–3.1753(17) Å. Moreover, two Cu(1) atoms are connected by two Br(3) to generate another $[Cu_2Br_2]$ units with Cu–Cu distance of 2.8299(15) Å. Then, the $[Cu_4Br_5]^-$ and $[Cu_2Br_2]$ subunits link each other via Br(4) and Br(3) atoms to form a

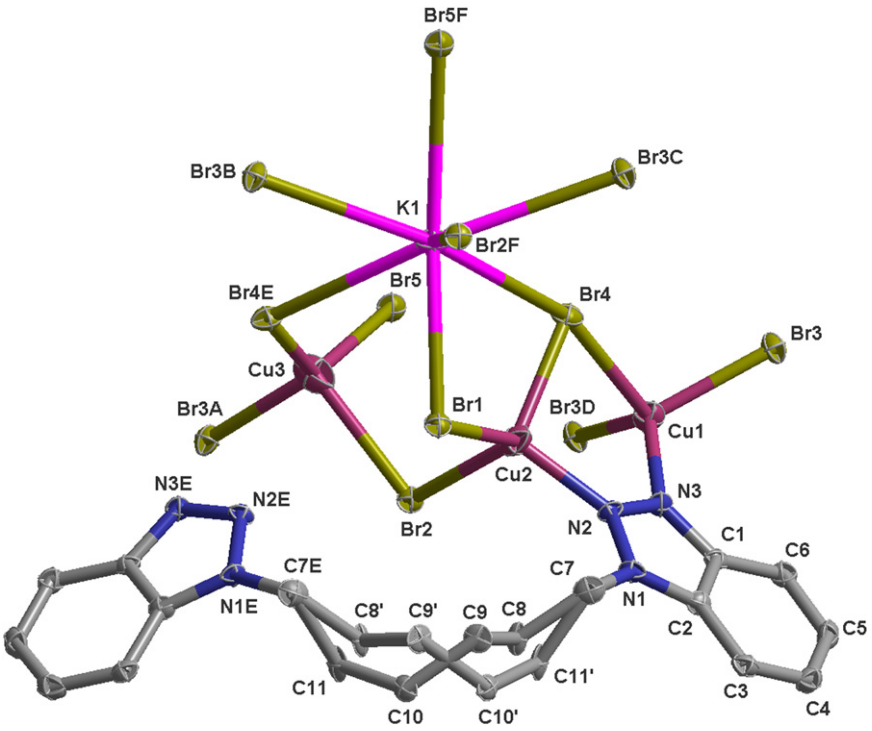

Fig. 3. View of the coordination environments for compound **2** [Symmetry codes: A—x, $0.5+y$, $-z$; B—$1-x$, $0.5+y$, $-z$; C—$1-x$, $-y$, $-z$; D—x, $-y$, $-z$; E—x, $0.5-y$, z; F—$1+x$, y, z].

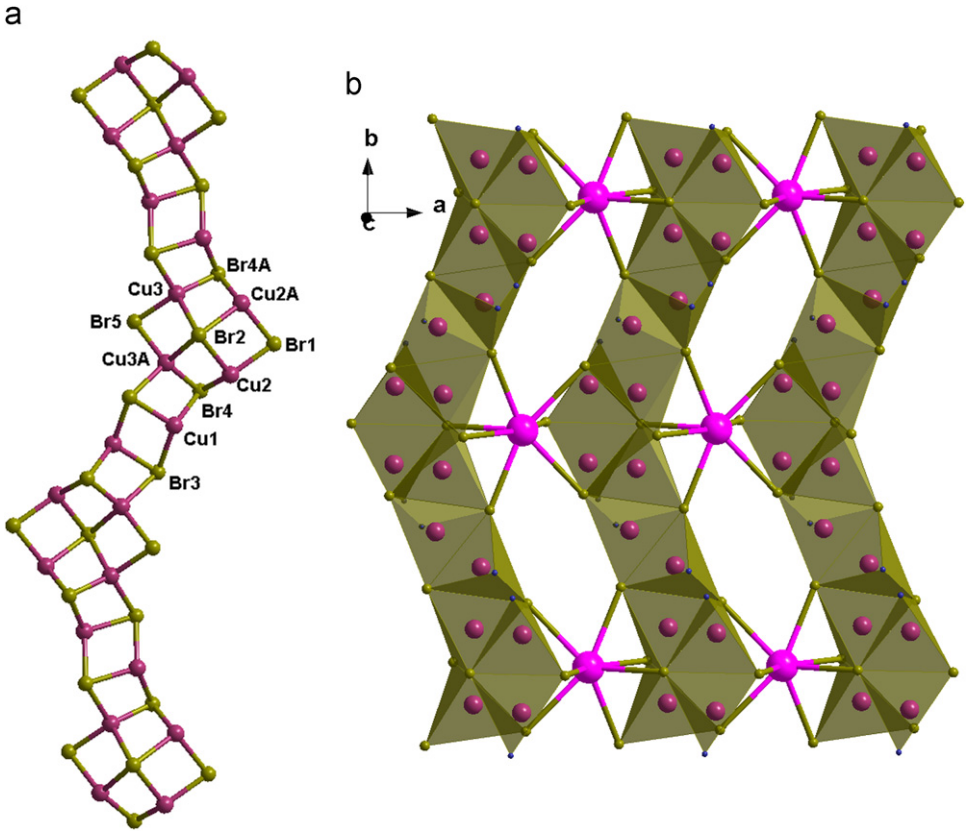

Fig. 4. View of 1D inorganic ribbon structure (left) and 2D hybrid layer (right) in compound **2**.

unique 1D $[Cu_6Br_7]^-$ anionic chain as depicted in Fig. 4 (left). Just like the *anti*-arrangement of $[Cu_6I_7]$ motifs in compound **1**, the orientation of two adjacent bow-shaped $[Cu_4Br_5]$ units is opposite. Furthermore, as shown in Fig. 4 (right), these 1D inorganic chains are connected by heptacoordinated K atoms to give a 2D neutral inorganic $[KCu_6Br_7]$ layer. In this layer, five

independent bromine atoms are of μ_3 (Br(1) and Br(5)), μ_4 (Br(3) and Br(4)) and μ_5 (Br(2)) bridging modes, respectively. Just like the 1D organic–inorganic hybrid chain of **1**, the unoccupied benzotriazole N atoms finish the tetrahedral sphere of Cu(1) and Cu(2) centers using the pyrazole-like bridging mode, which generates a $[Cu_2N_2Br]$ five-membered rings with copper separations of about 3.33 Å. Thus, each BBTH ligand takes the *cisoid*-configuration and acts as μ_4-bridge to link four copper atoms as depicted in Figure S2 (a). To the best of our knowledge, it is the first example that 1,6-Bi(benzotriazole)hexane was utilized to construct hybrid coordination polymers. The BBTH ligands alternately distribute on the two sides of the inorganic $[KCu_6Br_7]$ layer to give the 2D organic–inorganic hybrid network (Figure S2 (b) and (c)) for compound **2**. Ultimately, adjacent 2D hybrid layers was packed to present a 3D hybrid framework as shown in Fig. 5, through strong aromatic π–π stacking interactions between benzotriazole rings from adjacent layers, with a center-to-center distance of about 3.6 Å.

3.3. XRPD, FT-IR and TG/DTA

As shown in Figure S3, complexes **1** and **2** were characterized via X-ray powder diffraction (XRPD) at room temperature. The XRPD pattern measured for the as-synthesized samples were basically in consistent with the XRPD patterns simulated from the respective single-crystal X-ray data using the Mercury 1.4 program, which indicate the purity of samples **1** and **2**. Whats more, on the basis of the XRPD results it can be established that the single crystal selected is a representative of the bulk compound.

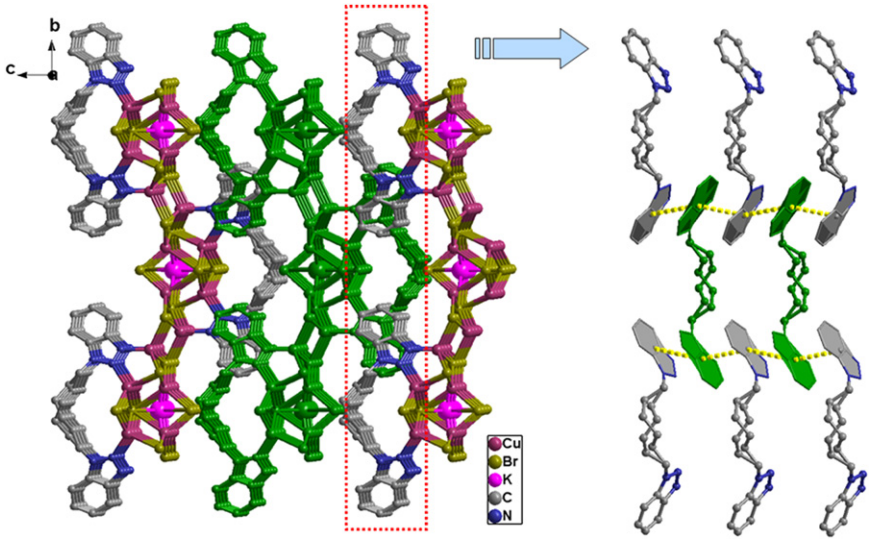

Fig. 5. View of 3D supramolecular architecture packed through strong aromatic π–π stacking interactions between benzotriazole rings from adjacent hybrid layers for **2**.

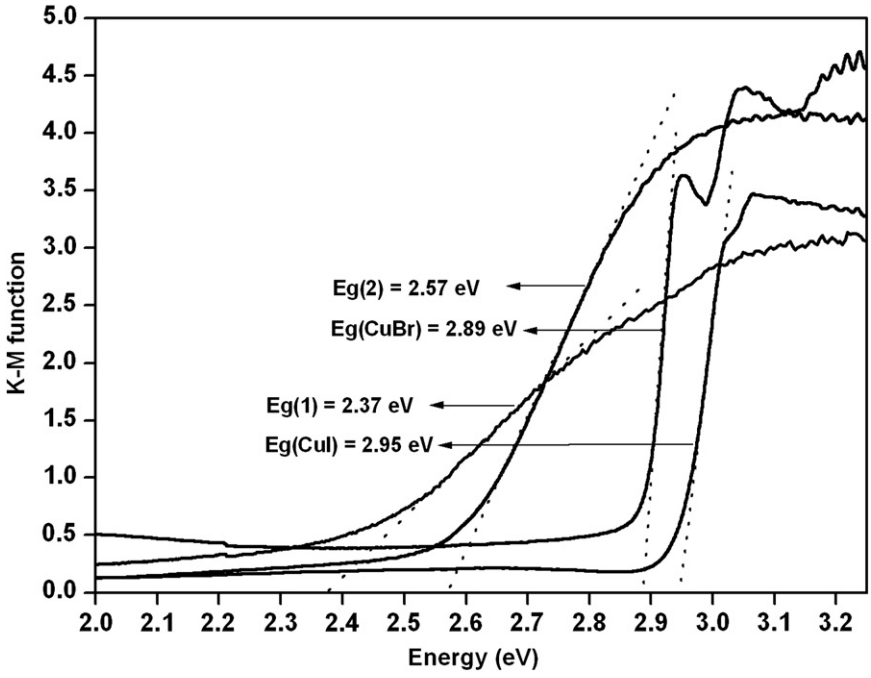

Fig. 6. Optical absorption spectra for solid samples of **1** and **2**.

Since BBTH ligand has been ruptured during the synthesis of complex **1**, we should only select benzotriazole (BTA) as the comparison instead of BBTH ligand, when the FT-IR spectra of hybrid complex **1** was studied (Figure S4 (a)). Three absorption bands at 2973, 1446 and 1380 cm^{-1} are attributed to the flex vibration of methyl, while one absorption band at 2925 cm^{-1} is attributed to the flex vibration of methylene among complex **1**, which indicates the rupture of the ligand and the existence of methyl and methylene. Whats more, the framework vibrations of phenyl and triazole rings are both in the range of 1200–1600 cm^{-1}. The difference in the range of 1000–1300 cm^{-1} shows that nitrogen atoms of benzotriazole rings have coordinated with copper atoms. The FT-IR spectra of BBTH ligand and hybrid complex **2** are similar to each other as shown in Figure S4 (b). Two absorption bands at 2934 and 2854 cm^{-1} (2937 and 2859 cm^{-1} for BBTH) are attributed to the flex vibration of methylene. The framework vibrations of phenyl and triazole rings are in the range of 1200–1600 cm^{-1}. The slightly difference in the range of 1000–1300 cm^{-1} shows that nitrogen atoms of benzotriazole rings have coordinated with copper atoms.

Due to the importance of thermal stability for organic–inorganic hybrid materials, complexes **1** and **2** were studied by thermal analysis under an air atmosphere from 40 to 1000 °C (Figure S5). The weight loss curve of complex **1** shows that it is stable up to ca. 150 °C. There are two weight loss steps occurred between 150 and 900 °C. The first weight loss observed between 150 and 330 °C, resulted from the decomposition of ETA ligand (exptl: 23.7%, calcd: 24.8%). The second weight loss corresponded to the loss of iodine anions (exptl: 54.2%, calcd: 53.9%). The weight loss curve of complex 2 shows that it is stable up to ca. 330 °C, over the range 330–400 °C, a sharp weight loss was due to the decomposition of BBTH (exptl: 25.8%, calcd: 24.6%). In the temperature range 400–950 °C, a mild weight loss process is ascribed to the sublimation of CuBr. This conclusion is supported by the value of the second weight loss (exptl: 69.4%, calcd: 71.4%).

3.4. Study of optical band gap

In order to explore the conductivity of the two compounds **1** and **2**, the measurements of diffuse reflectivity for powder crystal

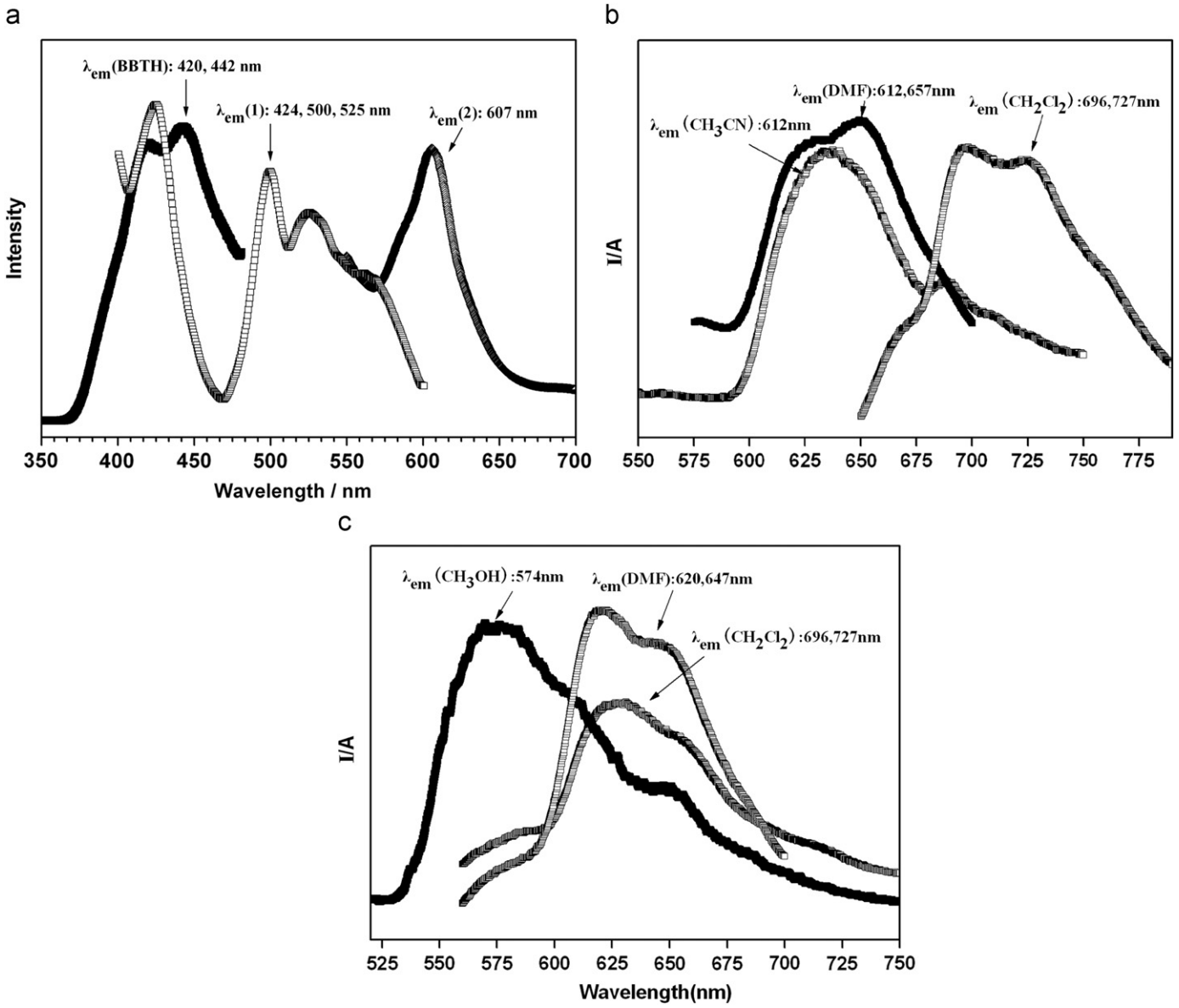

Fig. 7. Solid state (a) and solution (b and c) emission spectra of **1** and **2**.

samples were used to obtain their band gap (E_g). The band gap E_g was determined as the intersection point between the energy axis and the line extrapolated from the linear portion of the absorption edge in a plot of Kubelka–Munk function F against energy E [47,48]. Kubelka–Munk function, $F=(1-R)^2/2R$, was converted from the recorded diffuse reflectance data, where R is the reflectance of an infinitely thick layer at a given wavelength. The F versus E plots for the compounds are shown in Fig. 6, and the E_g values assessed from the steep absorption edge is 2.37 and 2.57 eV, respectively, which indicate that both hybrid compounds are potential semiconductor materials. It should be noted that these band gap sizes are significantly smaller than that of CuBr and CuI (2.89 eV for CuBr and 2.95 eV for CuI) (Fig. 6) [49].

3.5. Photoluminescence properties

It is well know that the copper(I) halide complexes with both discrete and multi-dimensional structure show excellent luminescence properties [50–55]. Thus, we reported herein the photoluminescence of the two compounds in the solid state under room temperature. To understand more thoroughly the nature of these emission bands, the luminescence of BBTH was also investigated. The intraligand emission of the free BBTH was observed at 442 nm along with a shoulder band at 420 nm ($\lambda_{ex}=290$ nm). As shown in Fig. 7, upon excitation of the solid sample **1** at 370 nm, a series of intense bands in the emission spectra are observed in the range of 400–600 nm, peaking at 424, 500 and 525 nm, respectively. In our opinion, the band at 424 nm should attributed to the intraligand transitions, and the emission bands at 500 and 525 nm are tentatively assigned to ligand-to-metal charge transfer (LMCT) between the Cu(I) atoms and the ligands. The emission spectra of 2 in the solid state have a maximum at approximately 607 nm, upon excitation at 493 nm. Thus, the clear red shift of the emission band of **2** compared to that of the free BBTH molecule may also originate from the excited states of ligand-to-metal charge transfer (LMCT) [6,55].

Usually, it has poor solubility in most organic solvents for the crystals which are synthesized by hydrothermal or solvothermal reaction [56]. To investigate the influence of common organic solvents on the luminescent property of **1** and **2**, the effects of several solvents with different molecular sizes and polarity on the maximum fluorescent wavelengths were studied. It was found that the maximum fluorescent wavelengths of **1** in different solvents followed the order CH_2Cl_2, Dimethylformamide (DMF) and acetonitrile (CH_3CN), while the maximum fluorescent wavelengths of **2** in different solvents followed the order CH_2Cl_2, DMF and methanol (Fig. 7), which show that the maximum fluorescent wavelengths varies with the polarity of solvents. The solvent-dependent fluorescence properties of the framework can be attributed to the effect of solvent polarity. Thus, the results have shown that the maximum fluorescence wavelengths in the several solvents were blue-shifted when the polarity of solvents solution was increased.

4. Conclusion

Using 1,6-Bi(benzotriazole)hexane flexible ligand and CuI or CuBr, we have successfully synthesized two novel coordination polymers constructed from novel $[Cu_6I_7]_n^{n-}$ anionic chain motifs and characterized roundly as well. Based on this work, further investigations on other flexible benzotriazole ligands and metal halide or pseudohalide substructures are currently processed in our lab.

Supplementary material

Crystallographic data have been deposited with the Cambridge Crystallographic Data Center (CCDC) (E-mail: deposit@ccdc.cam.ac.uk) as supplementary materials and the CCDC reference numbers is 750885 for **1** and is 750886 for **2**.

Acknowledgment

This work was supported by the National Natural Science Foundation of China (grant Nos. 20801033 and 20871079), the Natural Science Foundation of Shaanxi Province (2009JQ2003), the Youth Foundation of School of Chemistry and Materials Science, and the Innovation Funds of Graduate Programs, Shaanxi Normal University.

Appendix A. Supplementary data

The online version of this article contains additional supplementary data. Please visit doi:10.1016/j.jssc.2010.03.007

References

[1] O. Sato, T. Iyoda, A. Fujishima, K. Hashimoto, Science 271 (1996) 49–51.
[2] O.R. Evans, R.G. Xiong, Z.Y. Wang, G.K. Wong, W.B. Lin, Angew. Chem. Int. Ed. 38 (1999) 536–538.
[3] C. Janiak, S. Deblon, H.P. Wu, M.J. Kolm, P. Klüfers, H. Piotrowski, P. Mayer, Eur. J. Inorg. Chem. (1999) 1507–1521.
[4] E. Breuning, U. Ziener, J.M. Lehn, E. Wegelius, K. Rissanen, Eur. J. Inorg. Chem. (2001) 1515–1521.
[5] Z.B. Han, E.B. Wang, G.Y. Luan, Y.G. Li, H. Zhang, Y.B. Duan, C.W. Hu, N.H. Hu, J. Mater. Chem. 12 (2002) 1169–1173.
[6] J.H. Luo, M.C. Hong, R.H. Wang, Q. Shi, R. Cao, J.B. Weng, R.Q. Sun, H.H. Zhang, Inorg. Chem. Commun. 6 (2003) 702–705.
[7] N. Hao, F.C. Liu, E.B. Wang, R.D. Huang, Y.Q. Li, C.W. Hu, Inorg. Chem. Commun. 6 (2003) 728–732.
[8] X.J. Liu, Q.R. Fang, G.S. Zhu, M. Xue, X. Shi, G. Wu, G. Tian, S.L. Qiu, L. Fang, Inorg. Chem. Commun. 7 (2004) 31–34.
[9] H. Jin, C. Qin, Y.G. Li, E.B. Wang, Inorg. Chem. Commun. 9 (2006) 482–485.
[10] W.G. Wang, A.J. Zhou, W.X. Zhang, M.L. Tong, X.M. Chen, M. Nakano, C.C. Beedle, D.N. Hendrickson, J. Am. Chem. Soc. 129 (2007) 1014–1015.
[11] M.H. Alizadeh, M. Mirzaei, H. Razavi, Mater. Res. Bull. 43 (2008) 546–555.
[12] M. Eddaoudi, J. Kim, N. Rosi, D. Vodak, J. Wachter, M.O. Keeffe, O.M. Yaghi, Science 295 (2002) 469–472.
[13] O.R. Evans, W.B. Lin, Acc. Chem. Res. 35 (2002) 511–522.
[14] J.D. Lin, Z.H. Li, T. Li, J.R. Li, S.W. Du, Inorg. Chem. Commun. 9 (2006) 675–678.
[15] Z. Li, M. Li, S. Z Zhan, X.C. Huang, S.W. Ng, D. Li, Cryst. Eng. Commun. 10 (2008) 978–980.
[16] X.P. Zhou, S.H. Lin, D. Li, Y.G. Yin, Cryst. Eng. Commun. 11 (2009) 1899–1903.
[17] J.Y. Lu, B.R. Cabrera, R.J. Wang, J. Li, Inorg. Chem. 37 (1998) 4480–4481.
[18] P.M. Graham, R.D. Pike, Inorg. Chem. 39 (2000) 5121–5132.
[19] T. Wu, M. Li, D. Li, X.C. Huang, Cryst. Growth Des. 8 (2008) 568–574.
[20] K. Skorda, T.C. Stamatatos, A.P. Vafiadis, A.T. Lithoxoidou, A. Terzis, S.P. Perlepes, J. Mrozinski, C.P. Raptopoulou, J.C. Plakatouras, E.G. Bakalbassis, Inorg. Chim. Acta 358 (2005) 565–582.
[21] L.F. Jones, L.O. Dea, D.A. Offermann, P. Jensen, B. Moubaraki, K.S. Murray, Polyhedron 25 (2006) 360–372.
[22] S. Hu, A.J. Zhou, Y.H. Zhang, S. Ding, M.L. Tong, Cryst. Growth Des. 6 (2006) 2543–2550.
[23] Y. Wang, M.C. Hu, Q.G. Zhai, S.N. Li, Y.C. Jiang, W.J. Ji, Inorg. Chem. Commun. 12 (2009) 281–285.
[24] M.C. Hu, Y. Wang, Q.G. Zhai, S.N. Li, Y.C. Jiang, Y. Zhang, Inorg. Chem. 48 (2009) 1449–1468.
[25] M. Li, Z. Li, D. Li, Chem. Commun. (2008) 3390–3392.
[26] H. Zhou, P. Lin, Z.H. Li, S.W. Du, J. Mol. Struct. 881 (2008) 21–27.
[27] Y. Chen, H.X. Li, D. Liu, L.L. Liu, N.Y. Li, H.Y. Ye, Y. Zhang, J.P. Lang, Cryst. Growth Des. 8 (2008) 3810–3816.
[28] M. Knorr, F. Guyon, A. Khatyr, C. Daschlein, C. Strohmann, S.M. Aly, A.S. Abd-El-Aziz, D. Fortinc, P.D. Harvey, Dalton Trans. (2009) 948–955.
[29] S.B. Ren, L. Zhou, J. Zhang, Y.Z. Li, H.B. Du, X.Z. You, Cryst. Eng. Commun. 11 (2009) 1834–1836.
[30] C. Xie, L. Zhou, W.X. Feng, J.K. Wang, W. Chen, J. Mol. Struct. 921 (2009) 132–136.
[31] A.J. Lan, L. Han, D.Q. Yuan, F.L. Jiang, M.C. Hong, Inorg. Chem. Commun. 10 (2007) 993–996.

[32] Q.G. Zhai, X.Y. Wu, S.M. Chen, C.Z. Lu, W.B. Yang, Cryst. Growth Des. 6 (2006) 2126–2135.
[33] L.P. Wang, X.R. Meng, E.P. Zhang, H.W. Hou, Y.T. Fan, J. Organomet. Chem. 692 (2007) 4367–4376.
[34] X. Wang, L.K. Li, H.W. Hou, J. Wu, Y.T. Fan, Eur. J. Inorg. Chem. (2007) 5234–5245.
[35] R. Peng, S.R. Deng, M. Li, D. Li, Z.Y. Li, Cryst. Eng. Commun. 10 (2008) 590–597.
[36] W.J. Shi, C.X. Ruan, Z. Li, M. Li, D. Li, Cryst. Eng. Commun. 10 (2008) 778–783.
[37] Q.G. Zhai, M.C. Hu, Y. Wang, W.J. Ji, S.N. Li, Y.C. Jiang, Inorg. Chem. Commun. 12 (2009) 286–289.
[38] X.J. Xie, G.S. Yang, C. Lin, F. Wang, Huaxue Shiji 22 (2000) 222–223.
[39] G.M. Sheldrick, SADABS, program for area detector adsorption correction, Institute for Inorganic Chemistry, University of Göttingen, Germany, 1996.
[40] G.M. Sheldrick, SHELXL-97, Program for solution of crystal structures, University of Göttingen, Germany, 1997.
[41] J.K. Cheng, Y.G. Yao, J. Zhang, Z.J. Li, Z.W. Cai, X.Y. Zhang, Z.N. Chen, Y.B. Chen, Y. Kang, Y.Y. Qin, Y.H. Wen, J. Am. Chem. Soc. 126 (2004) 7796–7797.
[42] M. Vitale, P.C. Ford, Coord. Chem. Rev. 219–221 (2001) 3–16 and references therein.
[43] A. Vega, J.Y. Saillard, Inorg. Chem. 43 (2004) 4012–4018.
[44] M. Sarkar, K. Biradha, Chem. Commun. (2005) 2229–2231.
[45] S. Hu, M.L. Tong, Dalton Trans. (2005) 1165–1167.
[46] J.G. Haasnoot, Coord. Chem. Rev. 131 (2000) 200–202.
[47] J.I. Pankove, Optical Processes in Semiconductors, Prentice-Hall, Englewood Cliffs, New Jersey, 1971.
[48] W.M. Wesley, W.G.H. Harry, Reflectance Spectroscopy, Wiley, New York, 1966.
[49] J.W. Cheng, S.T. Zheng, G.Y. Yang, Inorg. Chem. 46 (2007) 10261–10267.
[50] H.W. Hou, X.R. Meng, Y.L. Song, Y.T. Fan, Y. Zhu, H.J. Lu, C.X. Du, W.T. Shao, Inorg. Chem. 41 (2002) 4068–4075.
[51] X.L. Zhou, X.R. Meng, W. Cheng, H.W. Hou, M.S. Tang, Y.T. Fan, Inorg. Chim. Acta. 360 (2007) 3467–3474.
[52] P.C. Ford, E. Cariati, J. Bourassa, Chem. Rev. 99 (1999) 3625–3647.
[53] V. Wing, W. Yam, K. Kam, W. Lo, Chem. Soc. Rev. 28 (1999) 323–334.
[54] R.B. Zhang, J. Zhang, Z.J. Li, J.K. Cheng, Y.Y. Qin, Y.G. Yao, Cryst. Growth Des. 8 (2008) 3735–3744.
[55] H. Jin, C. Qin, Y.G. Li, E.B. Wang, Inorg. Chem. Commun. 9 (2006) 482–485.
[56] F. Wang, R.M. Yu, Q.S. Zhang, Z.G. Zhao, X.Y. Wu, Y.M. Xie, L. Qin, S.C. Chen, C.Z. Lu, J. Solid State Chem. 182 (2009) 2555–2559.